Study of structure-property relationship in steels based on analysis of EBSD data

Study of structure-property relationship in steels based on analysis of EBSD data

O A Chikova[1,2], D S Chezganov[1], V V Yuzhakov[1] and N I Sinitsin[1]

[1]Ural Federal University, 620002 Ekaterinburg, Russia
[2]Ural State Pedagogical University, 620017 Ekaterinburg, Russia

O.A.Chikova@urfu.ru

Abstract. In this work, we formulate novel data-driven assays for exploring the structure-property linkages for high-manganese austenitic wear-resistant steel 110G13L (Hadfield steel). Steel 110G13L has the following chemical composition, wt.%: C(0.95-1.50)-Mn(11.5-15.0). These assays are built on recent advances in high resolution quantification of material structure using correlations and principal analyses of electron backscatter diffraction (EBSD) data, as well as in the mechanical characterization using nanoindentation. These novel protocols are demonstrated on a steel 110G13L that exhibits various polycrystalline microstructures. A comparative analysis of EBSD data was carried out for samples of manganese steel 110G13L obtained by various methods. Analysis of the diffraction patterns of backscattered electrons allowed us to plot orientation maps, Schmid factor maps and distributions for austenite dendrites. Schmid factor maps are used to determine the degree of homogeneity of a possible deformation. The results of the measurement of hardness and Young's modulus for the austenite dendrites indicate the heterogeneity of the mechanical properties of the material in submicro-volumes due to lattice defects (dislocations) inside the crystallites.

1. Introduction

The structure-property linkages are leading to the development and deployment of advanced materials in emerging technologies [1]. In this work, we formulate novel data-driven assays for exploring the structure-property linkages for high-manganese austenitic wear-resistant steel 110G13L (Hadfield steel). Hadfield steel is known for its high hardness and wear resistance and is characterized by a content of 0.95-1.50 wt.% carbon and 11.5-15.0 wt.% manganese. In this paper, the results of a comparative electron backscatter diffraction (EBSD) study of crystalline structure of 110G13L steel ingots crystallized after heating to 1450 and 1630 °C are presented. Previously, the authors found that the heating of the 110G13L liquid steel to a temperature above 1630°C led to the destruction of microheterogeneity and change in conditions of metal crystallization [2]. Microheterogeneity of 110G13L liquid steel is understood as the presence of dispersed particles, which enriched by manganese, carbon and separated by interfacial surface from the melt. The relationship between destruction of the microheterogeneity state of the liquid steel 110G13L and changes in crystalline structure were investigated. These assays are built on recent advances in high resolution quantification of material structure using correlations and principal analyses of EBSD data, as well as in the mechanical characterization using nanoindentation [3-5].

The EBSD method allows revealing the structure of the studied material with subsequent quantitative processing of the images, obtaining the size and misorientation angle distribution of the structural element boundaries, estimating the proportion of low-angle and special grain boundaries of the material,

and plotting a Schmid factor map and a misorientation histogram of the grains [3-5]. Schmid factor maps are used to determine the degree of homogeneity of a possible deformation. The effects of an inhomogeneous stress-strain state and the criteria for failure and wear of Hadfield steel based on an analysis of EBSD data are discussed in Refs. [6-9]. In particular, it was shown that twinning and dislocations play a key role in the strengthening of Hadfield steel [7]. An increase in grain size can increase the strength of austenitic steels with a high Mn content without compromising their ductility and toughness at low temperature [8]. A relationship between wear and crystallographic orientation of individual grains for high-manganese steel was established [10].

2. Experimental

The comparative analysis of EBSD data for samples of manganese steel 110G13L obtained by various methods (heating the melt to 1450 and up to 1630°C) was carried out. The ingots of steel 110G13L were crystallized at a rate of 0.2°C/s after heating the melt to 1450 and 1630°C. The chemical composition of Hadfield steel samples was determined using a SPECTROMAX (Spectro Analytical Instruments GmbH, Germany) emission spectrometer: C – 1.2%, Si – 0.5%, Mn – 12.6%, Cr – 1.2%, Ni – 0.2%, and Fe – the rest.

The analysis of the sample crystal structure was performed by EBSD using a scanning electron microscope (SEM) AURIGA CrossBeam workstation (Carl Zeiss, Germany) equipped with HKL Channel 5 EBSD analysis system (Oxford Instruments, UK). The EBSD data were acquired by Flamenco Acquisition software (Oxford Instruments, UK) using the SEM operated at the accelerating voltage of 20 kV and electron beam current of 5nA. The sample surface was prepared by diamond polishing down to 1 μm with a final polishing by colloidal silica SF1 (Logitech, UK). The areas with sizes of 21×21 μm^2 were scanned with a step size of 60 nm. The obtained data were processed and analysed by Tango software (Oxford Instruments, UK).

The mechanical properties (Young's modulus E, hardness H) were measured by nanoindentation method using NanoScan-4D (FSBI "TISNCM", Russia) following requirements of ISO 14577. The measurements were performed under continuous loading conditions with a linearly increasing load up to 50 mN at room temperature. The loading and unloading of the indenter, as well as the recording of the P-h diagram (applied load – depth of the indention) were carried out automatically. The hardness and Young's modulus of dendrites were determined as a result of 50 measurements for each of the regions. The size of the indenter footprint was measured at a maximum depth of indenter. The method of Oliver and Farah was used to process the results of mechanical material testing [11].

3. Results and discussion

The optical images of the microstructure of Hadfield steel ingots crystallized after heating the melt to 1450 and 1630°C are shown in Figure 1. The microstructure of the ingots is represented by austenite dendrites, the interdendrite space is filled with a ferrite-pearlite mixture with carbides and carbonitrides. The grain size and the distance between the secondary branches of dendrites differ slightly from one sample to another. Nonmetallic inclusions, such as sulfides (FeS+MnS), nitrides, oxides, and oxysulfides, are present both at the boundaries and grain body. The Mn heterogeneity of austenite dendrites was found for the ingot superheated to 1630°C before crystallization resulting in segregation upon solidification. During Electrical Discharge Machining (EDM) of Hadfield steel, a segregation layer with increased manganese content on the treated surface was observed earlier [12]. In addition, carbides were not found at the grain boundaries, which indicates a chemical composition alignment in dissolution. The decomposition of austenite at the boundaries of dendrites was not revealed for ingot superheated up to 1630°C as well. The porosity for the ingot overheated to 1630°C was greater than for the rest one.

The EBSD study of the crystal structure of austenite dendrites for ingots crystallized after heating the melt to 1450 and 1630°C are presented in the form of inverse pole figure (IPF) orientation maps, Schmid factor maps, and distributions (Fig. 2). EBSD analysis allows obtaining the distribution of the structural element (crystallite) boundaries according to the angle of misorientation at the IPF maps. The concept of grain in EBSD analysis is different from that in traditional optical microscopy. Two adjacent

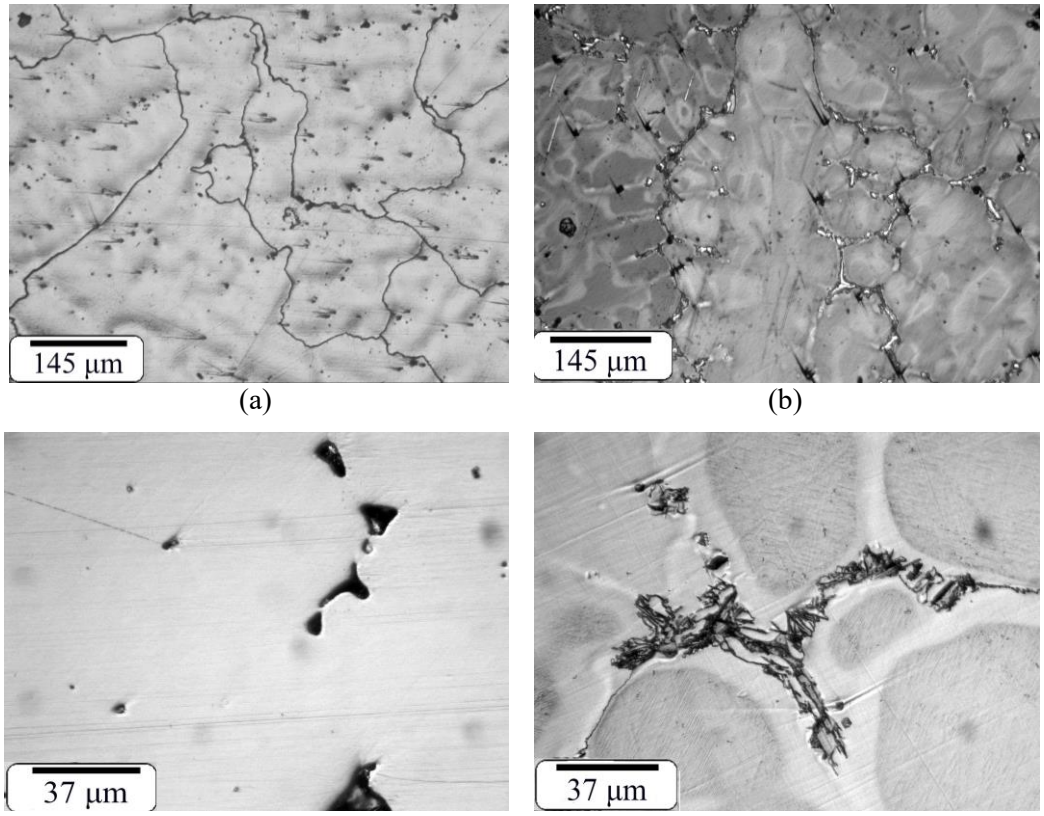

(a) (b)

(c) (d)

Figure 1. Microstructure of 110G13L steel ingots (optical microscopy): (a,c) crystallized after heating the melt to 1450°C; (b,d) crystallized after heating the melt to 1630°C.

points are considered to belong to the same crystallite, if the misorientation between them does not exceed the tolerance angle (subgrain structure) for all the studied samples. The Schmidt factor maps were plotted for a slip system typical for FCC crystals: (111) [110] with loading direction parallel to OZ axis. The distributions of the Schmid factor for samples made after heating of the melt to 1450 and 1630°C have one maximum, which indicates the homogeneity of its elastic characteristics (Fig. 2). The authors [13] investigated the mechanism of the formation of cast structures in Hadfield steel depending on changes in the cooling rate of the casting in two temperature ranges: crystallization (1200-1390°C) and separation of excess phases (560-790°C). A change in the cooling rate leads to decrease in the amount of excess phase (eutectic and carbides), change in their quantitative ratio and morphology. Such changes in the microstructure are reflected in changes in the magnitude of developing stresses. Thus, the features of the microstructure and crystalline structure characteristic of Hadfield steel ingots crystallized after the microheterogeneous state of the melt are destroyed similarly to the effects of changes in the cooling rate of the casting in the temperature range of the separation of excess phases.

It has been previously revealed that if almost all the boundaries are low-angle, the texture is stronger, than the Young's modulus and crystallite hardness is lower. The decrease in the modulus of elasticity due to high material texture significantly improves mechanical workability of the ingot [4].

The results of the measurement of mechanical properties are presented in Figure 3 and Table 1. For the austenite dendrites, there is no pronounced peak in the histograms corresponding to the average values of hardness and Young's modulus (Fig. 3). This type of E and H histograms indicates the heterogeneity of the mechanical properties of the material in submicro-volumes due to lattice defects (dislocations) inside the crystallites [4,14]. The interdendritic space has a complex structure (Fig. 1), which leads to heterogeneity of the mechanical properties of the material in submicro-volumes (Table 1). According to Ref. [14], the value of additional pressure, appeared at the interface between

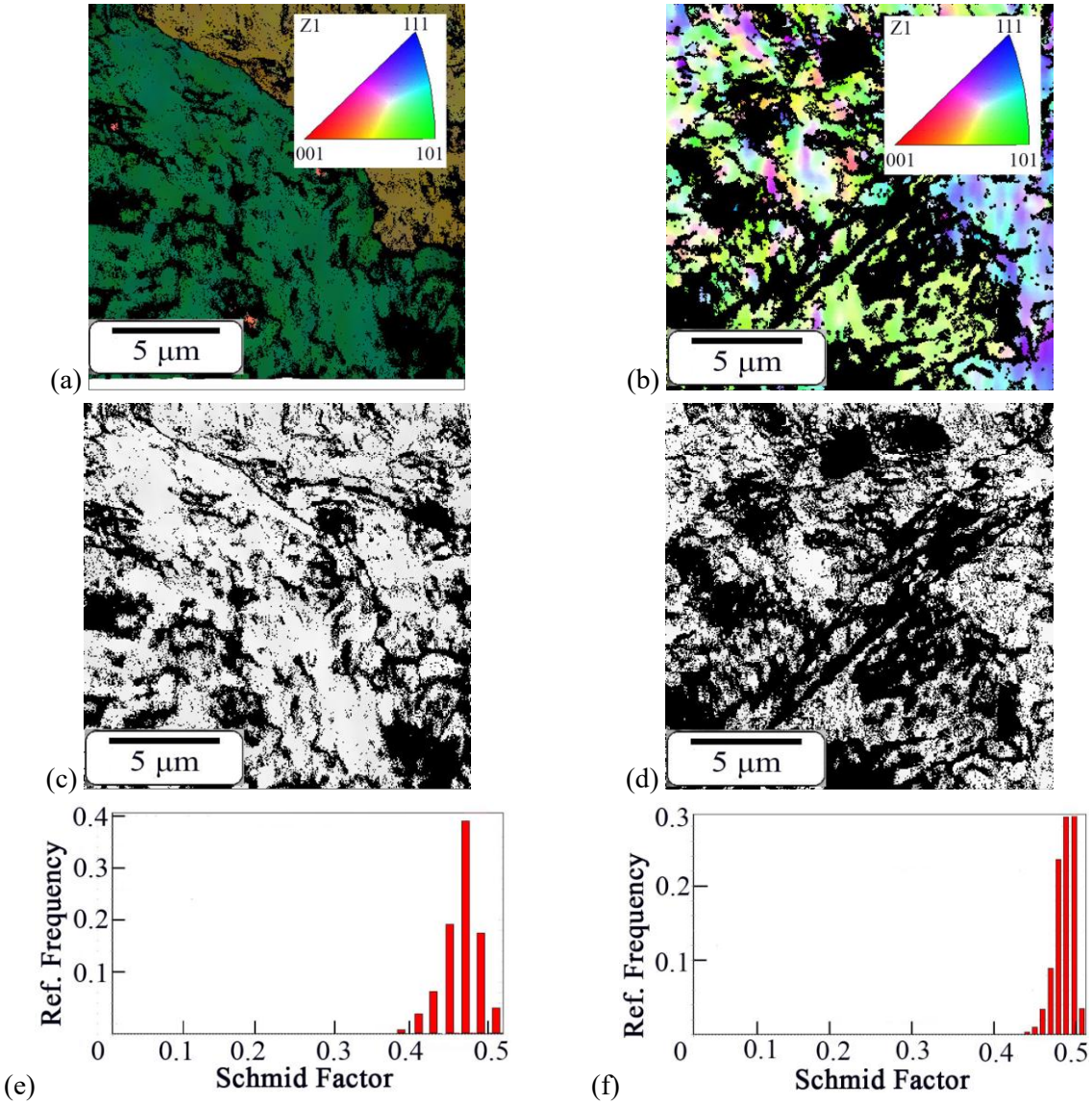

Figure 2. (a,b) IPF orientation maps; (c,d) Schmid factor maps; (e,f) Schmid factor distributions; (a,c,e) crystallized after heating the melt to 1450°C; (b,d,f) crystallized after heating the melt to 1630°C.

Table 1. Hardness and Young's modulus.

Material	Melt heating (°C)	H (GPa)	E (GPa)
The austenite dendrites	1630	4.7± 0.4	187 ± 6
The interdendrite space	1630	6.8 ± 0.7	101 ± 7
The segregation layer with increased manganese content in austenite dendrites	1630	11.6± 0.5	229±14
The austenite dendrites	1450	4.6± 0.2	174± 4

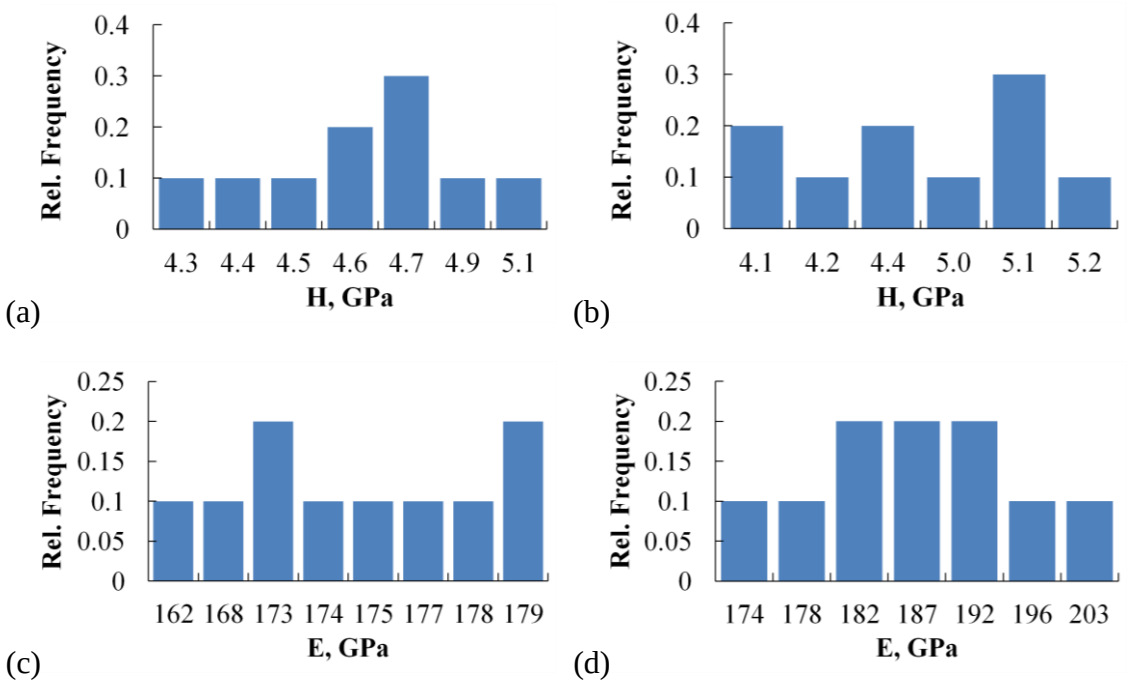

Figure 3. The distributions of (a,b) hardness H and (c,d) Young's modulus E of austenite dendrites for the ingots crystallized after heating the melts to (a,c) 1450°C and (b,d) 1630°C.

the segregation layer with increased manganese content and the body of austenite dendrites due to the difference in H and E, is significant and can cause the part to fail. Using the obtained values of the hardness and the Young's modulus of the body of austenite dendrites, the interdendritic space and the segregation layer with increased manganese content, the values of bonding strength and adhesion can be calculated [15].

4. Conclusion

A study was made of the relationship technology-structure-property based on analysis of EBSD data and nanoindentation for steel with a high content of manganese 110G13L (Hadfield steel). Steel 110G13L has the following chemical composition, wt.%: C(0.95-1.50)-Mn(11.5-15.0). A comparative analysis of EBSD and nanoindentation data was carried out for samples obtained by various methods. The samples crystallized at a rate of 0.2°C/s after heating the melt to 1450 and 1630°C. The results of the study of the structure of austenitic dendrites are presented using the basic analysis of EBSD data in the form of IPF maps, maps and histograms of Schmid factor. The results of measurements of mechanical properties in submicro-volumes by the nanoindentation method – hardness H (GPa) and Young's modulus E (GPa) - for austenitic dendrites, interdendritic space, segregation layer with a high content of manganese in austenitic dendrites are presented. EBSD data and nanoindentation data indicate the heterogeneity of the mechanical properties of the material in submicro-volumes due to lattice defects (dislocations) inside the crystallites.

Acknowledgements

The equipment of the Ural Centre for Shared Use “Modern nanotechnology” UrFU was used. The reported study was funded by RFBR (project No. 19-33-90198).

References

[1] Khosravani A, Cecen A and Kalidindi S R 2017 *Acta Mater.* **123** 55-69
[2] Chikova O A, Sinitsin N I and V’yukhin V V 2019 *Russ. J. Phys. Chem. A* **93** 1435-42

[3] Belonosov A V, Chikova O A, Yurovskikh V V and Chezganov D S 2013 *Russ. J. Nondestruct. Test.* **49** 196-205
[4] Chikova O A, Konstantinov A N, Shishkina E V and Chezganov D S 2013 *Russ. Metall.* **75** 35-44
[5] Chezganov D S, Chikova O A and Borovykh M A 2017 *Phys. Met. Metallogr.* **118** 857-63
[6] Harzallah R, Mouftiez A, Felder E, Hariri S and Maujean J-P 2010 *Wear* **269** 647-54
[7] Feng X, Zhang F, Zheng C, and Lü B 2013 *Sci. China Technol. Sci.* **56** 1151-4
[8] Wang X-J, Sun X-J, Song C, Chen H, Tong S, Han W and Pan F 2019 *Acta Metall. Sin. Engl.* **32** 746-54
[9] Machado P C, Pereira J I, Penagos J J, Yonamine T and Sinatora A 2017 *Wear* **376-7** 1064-73
[10] Li Y and Gu D 2014. *Mater. Des.* **63** 856-67
[11] Oliver W C and Pharr GM 2004 *J. Mat. Res.***19** 3-20
[12] Mouralova K, Benes L, Bednar J, Zahradnicek R, Prokes T, Matousek R, Hrabec P, Fiserova Z and Otoupalik J 2019 *J. Mech. Sci. Tech.* **33** 2371-86
[13] Gorlenko D, Vdovin K and Feoktistov N 2016 *China Foundry* **13** 433-42
[14] Chikova O A, Reznik P L and Ovsyannikov B V 2016 *Phys. Met. Metallogr.* **117** 1245-50
[15] Zhang C, Zhou H and Liu L 2014 *Acta Mater.***72** 239-51